J. Fluid Mech. (1990), *vol.* 213, *pp.* 171–189
Printed in Great Britain

Vortex-induced streamwise oscillations of a square-section cylinder in a uniform stream

By E. D. OBASAJU†, R. ERMSHAUS AND E. NAUDASCHER
Sonderforschungsbereich 210, 'Strömungsmechanische Bemessungsgrundlagen für Bauwerke', Universität Karlsruhe, West Germany

(Received 18 February 1988 and in revised form 8 August 1989)

The streamwise oscillation of a spring-mounted square-section cylinder set at angles of incidence, α, in the range from 0° to 45° is investigated in the reduced-velocity range $3 < U/ND < 13$ and Reynolds-number range from 3.2×10^3 to 1.4×10^4. The mass-damping parameter used for the investigations is 1.6 and this gives vibration amplitude up to $0.12D$. For small angles of incidence (i.e. $\alpha < 10°$), vibration occurs mainly near $U/ND = 1/2S$, where S is the Strouhal number for the stationary cylinder. In the neighbourhood of $\alpha = 13.5°$, which is where one of the separated shear layers is expected to reattach, vibration occurs near $U/ND = 1/S$. As α approaches 45° the amplitude observed near $U/ND = 1/S$ diminishes and small-amplitude vibration appears near $U/ND = 1/2S$.

At $\alpha = 0°$, vortices help to sustain oscillations by shedding when the cylinder is moving upstream. The mean drag of the oscillating cylinder drops and may reach less than half the stationary-cylinder value. When the amplitude of vibration is small, vortices of opposite sense of rotation are shed alternately and the familiar von Kármán vortex street is formed. For moderately high values of amplitude, two vortex patterns fundamentally different from that of the stationary cylinder are observed. Intermittently, pairs of vortices are then shed symmetrically from both sides of the cylinder. When this occurs a pair of contra-rotating vortices forms every cycle of the vibration. When vortices of opposite sign are shed alternately, one vortex from each side of the cylinder forms every two vibration cycles. In this latter case, it appears that each vortex is elongated and split into two parts. Split vortices of opposite sign pair up and then form a vortex street.

1. Introduction

Vortex shedding by an elastic cylinder can induce the cylinder to oscillate both transverse to and in the flow direction. If the axis of the cylinder is normal to the flow, which is a situation often encountered, oscillation commonly occurs transverse to the flow. Perhaps as a result of this, the majority of investigations into vortex-induced oscillations of cylindrical bodies has been concerned with this case. In comparison, very little is known on the case of streamwise oscillations of a cylinder.

Data for streamwise oscillation are available for the circular cylinder. This case has been reviewed by Griffin & Ramberg (1976), King (1977) and Bearman (1984). Let D be the cylinder diameter, U the free-stream velocity, N the frequency of streamwise vibration, and S the Strouhal number which, over a wide range of Reynolds number,

† On leave from the Department of Aeronautics, The City University, London EC1V 0HB, UK. Present address: BMT Fluid Mechanics Limited, Orlando House, 1 Waldegrave Road, Teddington, Middlesex TW11 8LZ, UK.

is about 0.2 for the stationary circular cylinder. Vibration occurs in two zones namely $1.0 < U/ND < 2.5$ and $2.5 < U/ND < 4.0$. It appears that the maximum amplitude of vibration that can occur is less than $0.2D$. When $U/ND < 2.5$, pairs of vortices are shed simultaneously and symmetrically from both sides of the oscillating cylinder. By contrast when $U/ND > 2.5$, vortices are shed alternately. Bearman (1984) has remarked that insufficient fundamental research has been carried out to fully explain the origin of the exciting force.

This paper describes one of a series of pilot experiments undertaken in order to provide insight into the mechanisms of excitation leading to streamwise oscillations. Work done so far in the program is reviewed in Naudascher (1987). Bluff bodies ranging from geometries with relatively weak vortex shedding, such as a sphere and a cylinder stub (i.e. a short circular cylinder with axis parallel to the flow), to geometries with strong shedding, such as plates and rectangular cylinders, have been examined. Preliminary results for spheres and cylinder stubs have been presented by Ermshaus, Knisely & Naudascher (1985). In this paper we shall concentrate on the square-section cylinder. The cylinder will be examined over a range of incidence from 0° to 45°, and the results of the investigation should complement the body of transverse oscillation data already available. The effect of incidence on the flow around a stationary square-section cylinder has been investigated by many workers including Lee (1975) and Obasaju (1983). If the undisturbed flow is smooth (i.e. turbulence level is less than about 1 %), then as the angle of incidence, α, is increased from 0°, one of the separated shear layers reattaches to a side face when the incidence is about 13.5°. At this incidence, the curve of Strouhal number versus α rises sharply to a maximum whereas the local steady drag coefficient drops to a minimum. In this paper, we shall investigate how the cylinder response changes as α is taken past this interesting point. We shall describe how the cylinder vibration modifies the vortex wake and shall attempt to identify the mechanism of excitation.

Some of our preliminary results for the square-section cylinder have been presented in Naudascher's (1987) general review. These show that flow-induced streamwise oscillation can, depending on the angle of incidence, occur when U/ND is either near $1/2S$ or near $1/S$. In the present paper, it is the vortex pattern generated by the vibrating cylinder that we find most remarkable. There are flow regimes where it appears that shed vortices are elongated and split into two parts. Split vortices of opposite sign pair up and then form a vortex street downstream of the cylinder. We shall estimate the vortex convection velocity, the cylinder drag and base pressure. Using this information in models of the vortex street, vortex strengths will be obtained. It will be seen that the strength of vortices shed during streamwise oscillations can be significantly less than the stationary cylinder value.

2. Experimental arrangement

Measurements were made in a low-speed wind tunnel with an open working section at the Institute of Hydromechanics, University of Karlsruhe, FRG. The turbulence level in the working section was about 0.5 %. The square-section cylinder was made of hard styrofoam. It had sides of $D = 60$ mm, length of $L = 683$ mm and was suspended horizontally by an arrangement of wires and springs, see figure 1. Great care was taken to ensure that the vibration characteristics of the model in still air were nearly linear. The amplitude was monitored with the aid of a small rectangular disc attached to the base of one of the supporting wires. The disc was sandwiched between two inductive coils which formed part of a carrier-frequency bridge. To

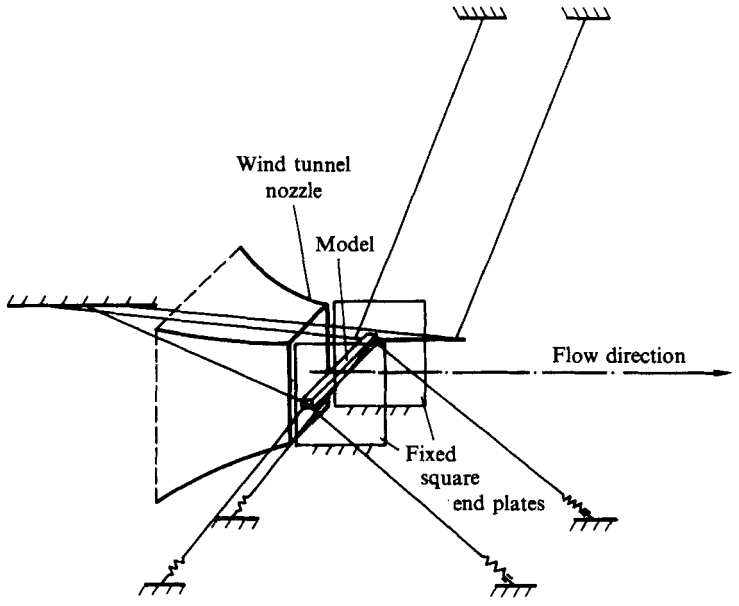

FIGURE 1. Experimental set-up.

reduce any influence of end effects, it was arranged for the cylinder to vibrate between two fixed square plates with sides of length 600 mm. The leading edge of each plate was carefully streamlined in order to avoid flow separation. The axis of the cylinder was located about 150 mm downstream of the plate leading edges and there were gaps of about 1 mm between the plates and the ends of the model.

The damping of the vibrating system was estimated from the decay of amplitudes during vibration in still air. In the incidence range 0° to 45°, the average value of the logarithmic decrement $\delta = 2\pi\zeta$, where ζ is the damping parameter, was 0.0027 and no systematic variation of δ with α was detected. The above value of δ includes a contribution due to flow generated by the vibrating model. Using Bearman *et al.* (1985) data for the streamwise force on a square-section cylinder in oscillating flow, this contribution was estimated to be about 0.0009 when the amplitude of vibration is $0.1D$. Hence the structural part of the damping is $\delta = 0.0018$. The equivalent mass of the vibrating system was estimated to be $M = 1.31$ kg. For $\delta = 0.0018$, this gives a mass-damping parameter, $K_s = \delta 2M/\rho D^2 L$, of 1.6 where L is the length of the cylinder and ρ is the fluid density.

The eigenfrequency of vibration, N, was about 4.6 Hz. The reduced velocity, U/ND, ranged from 3 to 13 giving a Reynolds number, $Re = UD/\nu$, where ν is the kinematic viscosity, in the range from 3.2×10^3 to 1.4×10^4. The flow in an axial plane through the mid-section of the cylinder was visualized using smoke. The smoke was illuminated by a sheet of light provided by a laser. This method is described in detail by Schmitt & Ruck (1986).

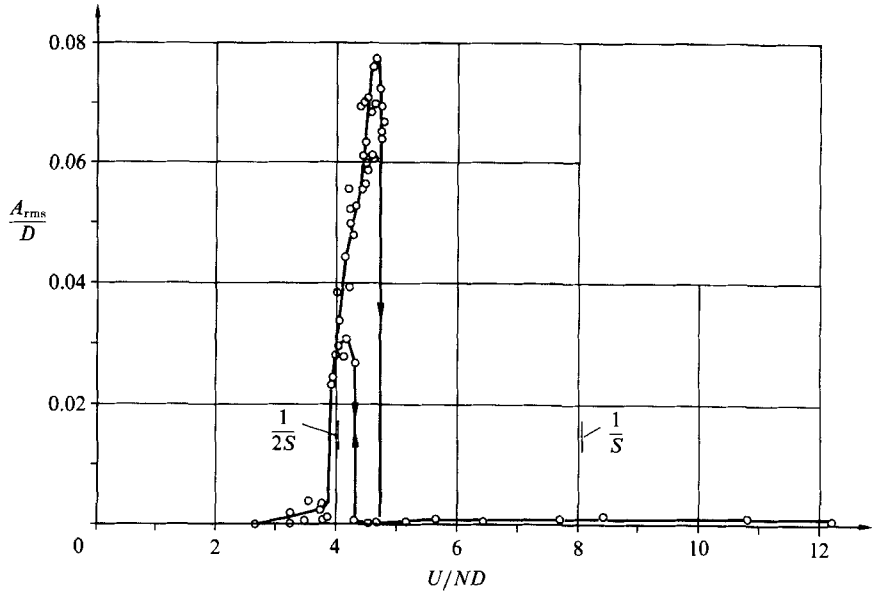

FIGURE 2. Root-mean-square value of cylinder amplitude, measured at $\alpha = 0°$, versus reduced velocity.

3. Experimental results

3.1. *Measurements of cylinder amplitude*

Figures 2–5 show the variation of the root-mean-square value of the cylinder amplitude with reduced velocity for different angles of incidence. The amplitudes were non-dimensionalized using the cylinder diameter D. The positions $U/ND = 1/S$ and $1/2S$ where the frequency of vibration N coincides with n and $2n$ respectively, where n is the frequency of vortex shedding from the stationary square-section cylinder, are indicated on each figure. Values of the Strouhal number for the stationary cylinder, S, were taken from Obasaju (1983), and these values agree closely with those of Knisely (1985) – see figure 6.

The response of the cylinder may be considered to be the result from three sources of excitation. First, there is a highly irregular background vibration generated by the unsteady buffeting loads induced by turbulence in the oncoming stream and in the wake of the cylinder. The contribution from this extraneous source of excitation increases continuously with U/ND, and reaches a maximum r.m.s. amplitude of about $0.003D$ at $U/ND \approx 12$. Far more significant is the oscillation due to other sources such as vortex- and movement-induced excitations. These usually occur in narrow ranges of U/ND near $1/S$ and $1/2S$, and the amplitudes depend on the angle of incidence. Maximum amplitude is attained at the high-reduced-velocity end of the range where vortex- and movement-induced oscillations occur. At maximum response, the modulation in the vibration amplitude is slight and the motion is closely sinusoidal. Vibration always occurs at practically the natural frequency $N = 4.6$ Hz. A change of 1 % in the frequency could have been detected easily with our apparatus.

The amplitude of the response near $U/ND = 1/S$ and $1/2S$ seems to depend on the degree of asymmetry in the mean position of the separated shear layers. For example, at $\alpha = 0°$ and 45°, the shear layers are symmetrical in the mean with

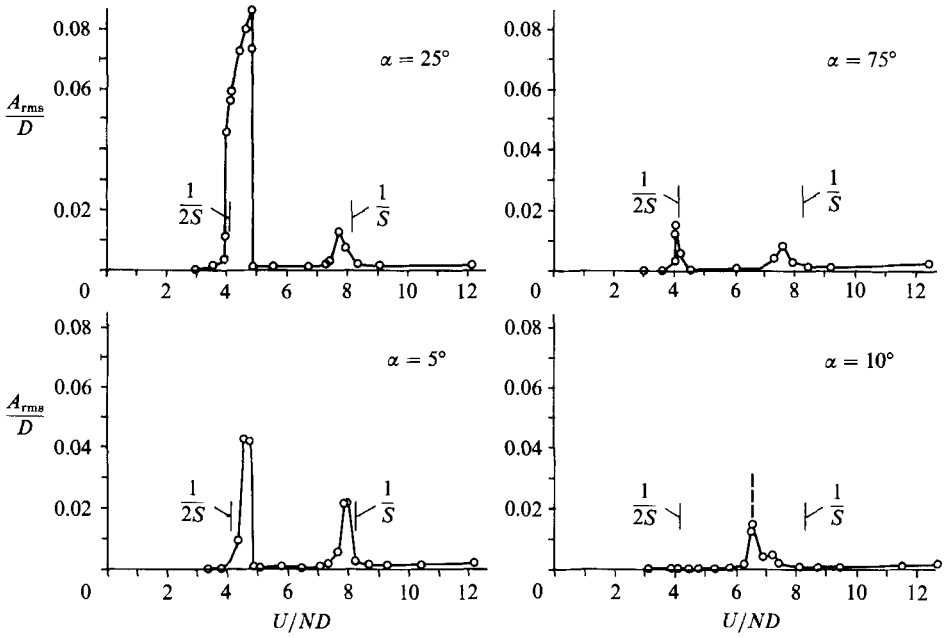

FIGURE 3. Root-mean-square value of cylinder amplitude versus reduced velocity.

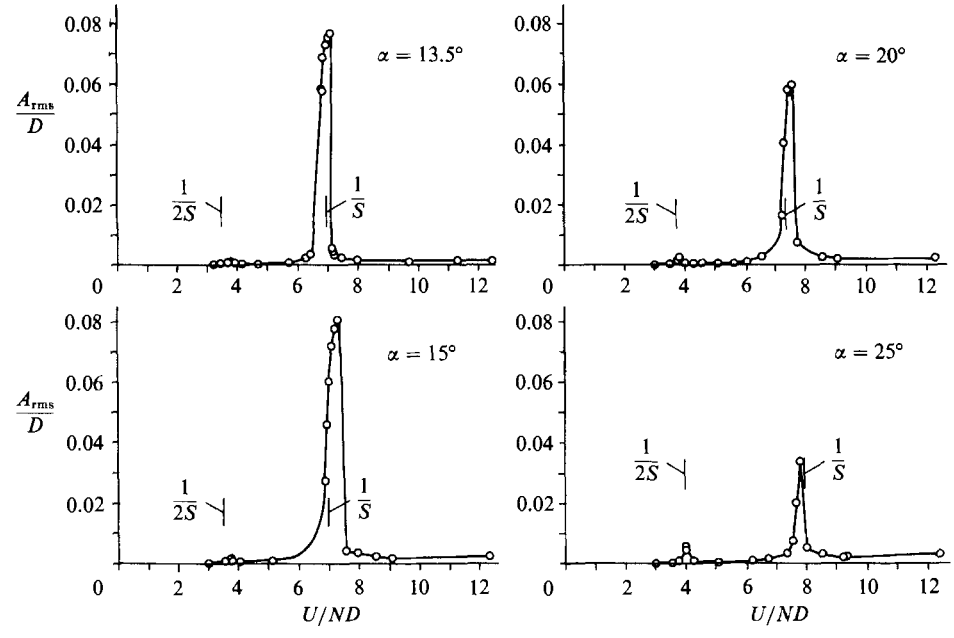

FIGURE 4. Root-mean-square value of cylinder amplitude versus reduced velocity.

respect to the wake centreline, and the response amplitude has a peak near $U/ND = 1.2S$, whereas there is only the weak background buffeting response near $U/ND = 1/S$. By contrast, one of the shear layers is expected to reattach near $\alpha = 13.5°$, and there is a strong peak in the amplitude near $U/ND = 1/S$ but only the background response near $1/2S$. It is interesting that for $\alpha = 10°$, Obasaju (1983)

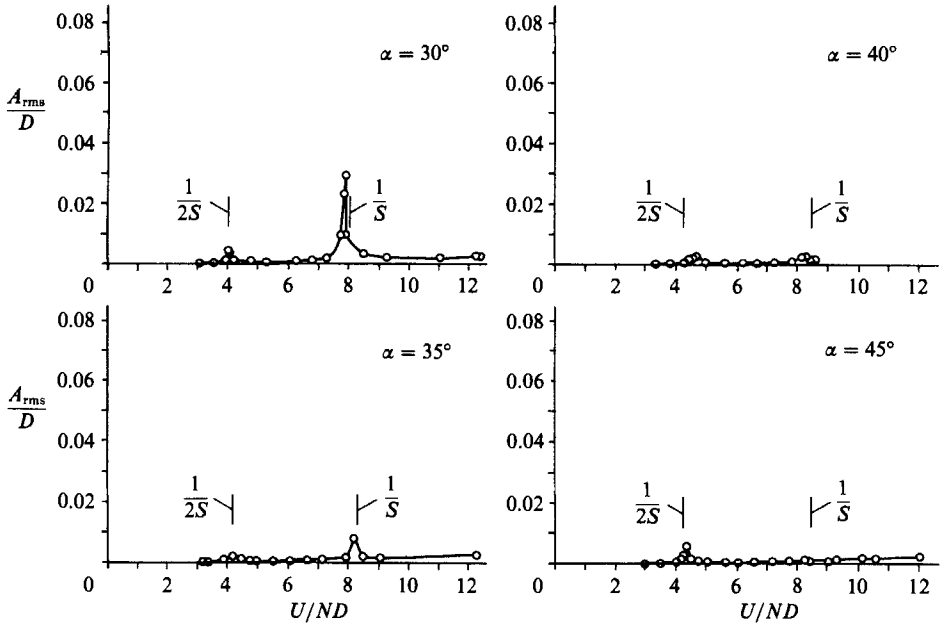

FIGURE 5. Root-mean-square value of cylinder amplitude versus reduced velocity.

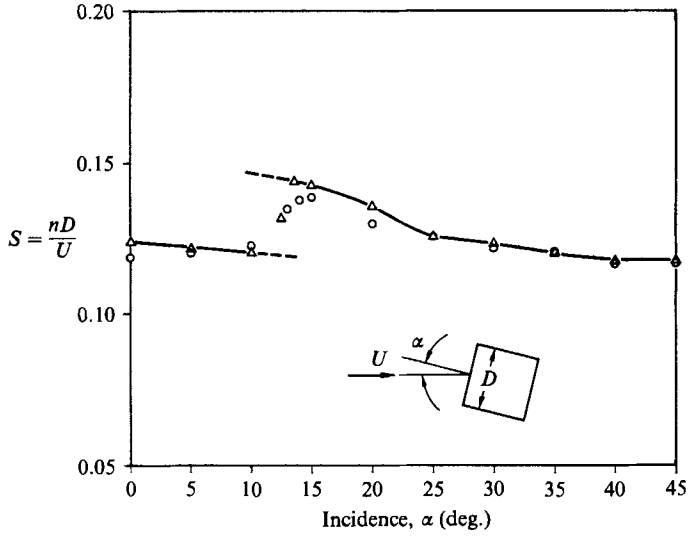

FIGURE 6. Strouhal number for the stationary square-section cylinder versus incidence: △, Obasaju (1983); ○, Knisely (1985).

data gave $1/S = 8.33$ but in our experiment higher-than-background response occurs in the range $6.5 \leqslant U/ND \leqslant 7.5$. Since for the reattached state of flow at $\alpha = 13.5°$, $1/S = 6.94$, it appears that during streamwise oscillation, reattachment occurs at lower than the expected angle of incidence.

Many sets of measurements were made at $\alpha = 0°$. These revealed that if U/ND is increased from about 4.0, the response amplitude can take one of two paths. For the conditions tested, one path leads to a maximum r.m.s. amplitude of about $0.03D$ and

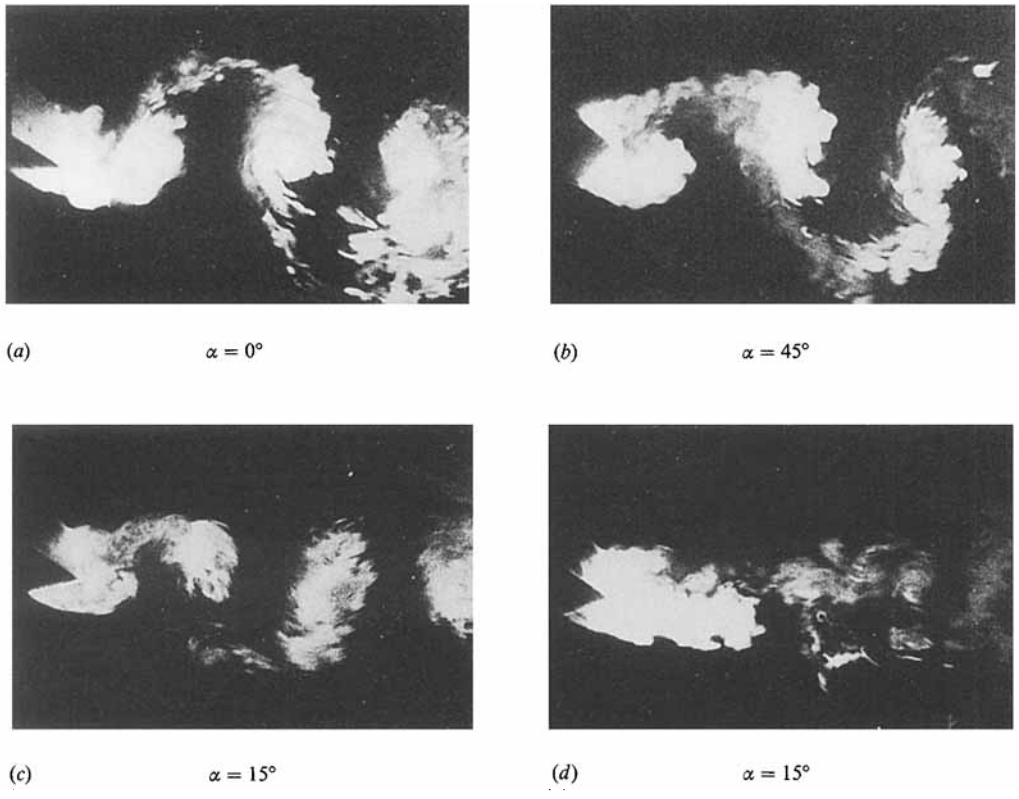

FIGURE 7. Vortex pattern behind a stationary square-section cylinder at $Re = 4.3 \times 10^3$.

a sharp drop in the cylinder amplitude at $U/ND \approx 4.25$ – see figure 2. The other path leads to a maximum r.m.s. amplitude of about $0.078D$ and a drop in amplitude at $U/ND \approx 4.75$. If the reduced velocity is between 4.25 and 4.75 and the cylinder is initially at rest, higher-than-background amplitudes of vibration can be produced if the cylinder is deflected to oscillate at a sufficiently high amplitude, namely $A/D \geqslant 0.2$. Attempts to produce higher-than-background oscillation by initial deflection were unsuccessful when U/ND is either below 3.8 or above 4.75.

Our results are described more fully in Ermshaus, Naudascher & Obasaju (1986).

3.2. *Estimation of mean drag*

Approximate measurements of mean drag were made at $\alpha = 0°$. The steady drag on the vibrating cylinder was estimated from the mean deflection of the model. The results are presented in terms of a drag coefficient $C_D = F/(\frac{1}{2}DL\rho U^2)$ where F is the steady drag force, U is the free stream velocity, and ρ is the fluid density; D and L are the diameter and length of the cylinder respectively. The values of C_D obtained in that fashion were 2.1, 1.5, 1.0, 1.2, 1.2, and 2.2 at $U/ND = 3.74$, 3.96, 3.99, 4.08, 4.19 and 4.37 respectively. During this set of experiments, the r.m.s. amplitude of vibration reached a maximum of about 0.03 and dropped to the background level at $U/ND \approx 4.3$. At $U/ND = 3.74$, the value of C_D is close to that of the stationary cylinder, see Obasaju (1983). As U/ND increases C_D decreases rapidly and settles at about half the stationary-cylinder value.

When vibration occurs transverse to the flow, the oscillating square-section

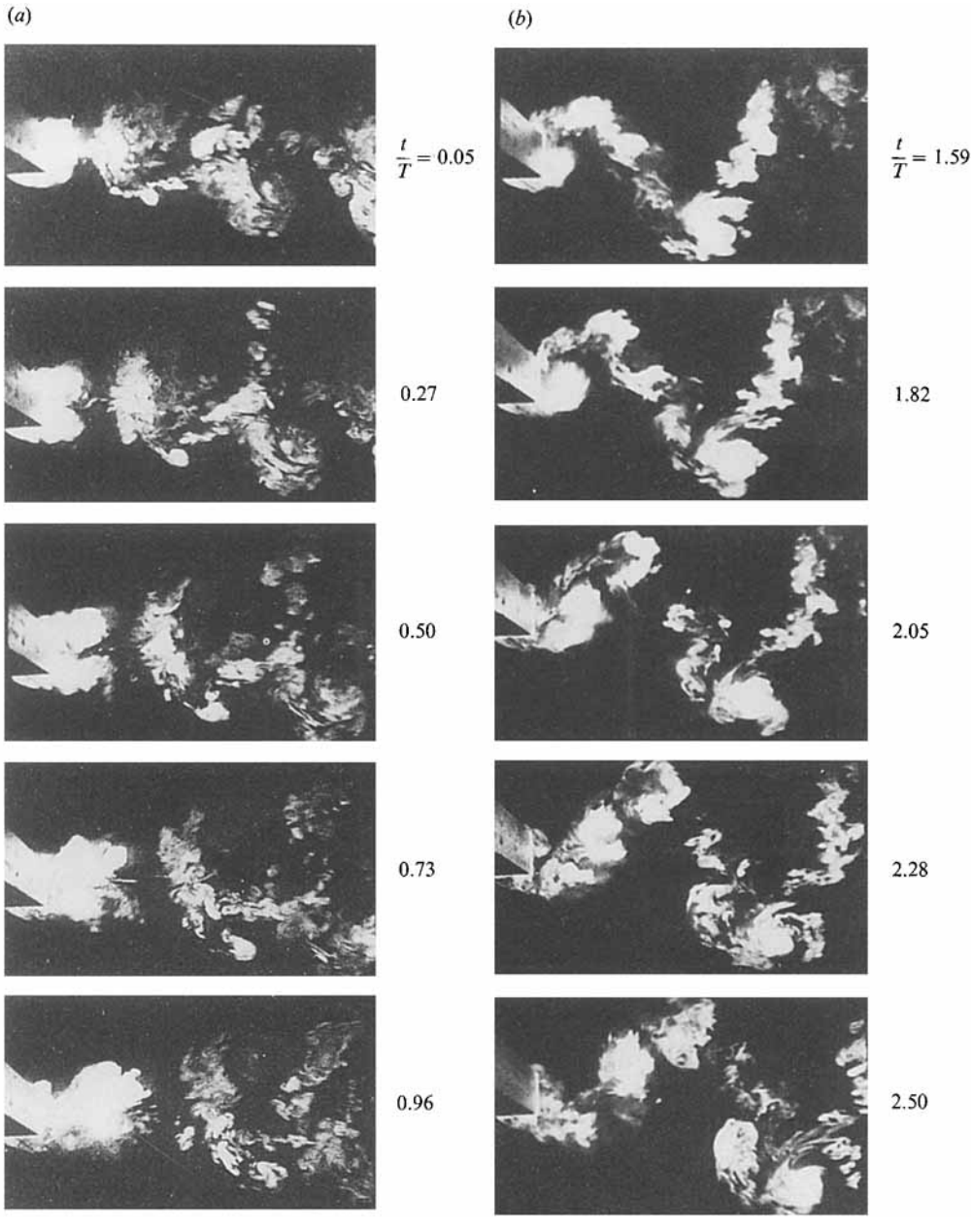

FIGURE 8(*a*, *b*). For caption see facing page.

cylinder mean drag has also been found to be less than the stationary-cylinder value. Bearman & Obasaju (1982) have reported that, at $U/ND \approx 4$, the oscillating square-section cylinder mean drag is down to about half of the stationary cylinder value when the amplitude of transverse oscillation is $0.1D$. Their pressure measurements show that the contribution of the front face of the model to the mean drag coefficient is about 0.8. Therefore for our present study, the base pressure coefficient, C_{pb}, is estimated to be $(C_D - 0.8)$. This means that during streamwise oscillation, C_{pb} can rise from the stationary-cylinder value of about -1.4 to as high as -0.2.

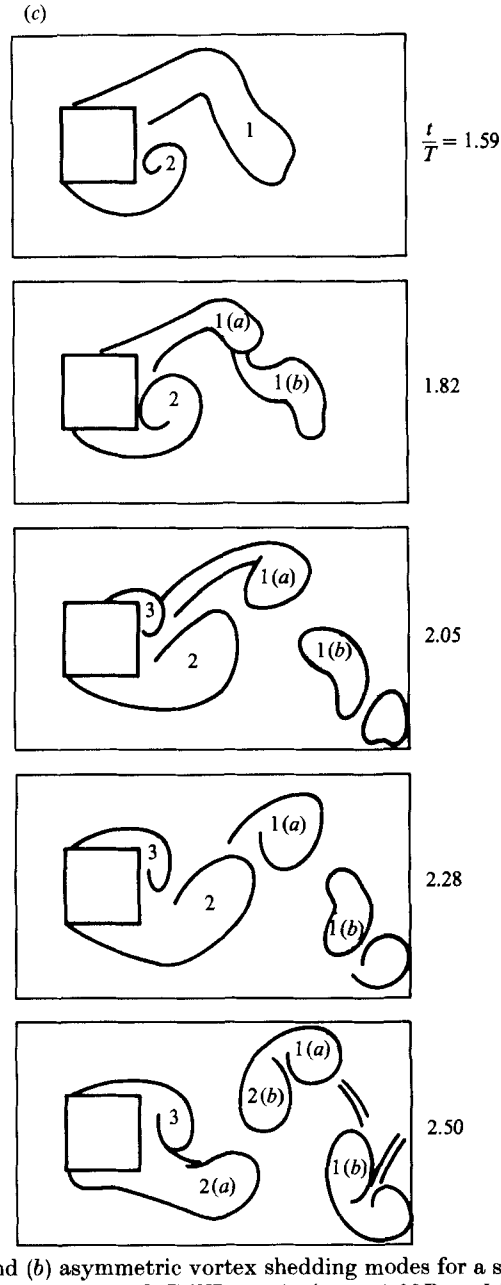

FIGURE 8. (*a*) Symmetric and (*b*) asymmetric vortex shedding modes for a square-section cylinder undergoing streamwise oscillations. $\alpha = 0°$, $U/ND = 4.0$, $A_{\text{rms}} = 0.03D$, and $Re = 4.3 \times 10^3$. T is the period and $t = 0$ when the cylinder is at its fully upstream position. (*c*) Sketches of vortex patterns for the asymmetric vortex shedding mode at $\alpha = 0°$, $U/ND = 4.0$, $A_{\text{rms}} = 0.03D$, $Re = 4.3 \times 10^3$.

3.3. *Flow visualization*

Smoke patterns recorded with the stationary model inclined at $\alpha = 0°$, 15°, and 45° are presented in figure 7. The field of view extends to about $8D$ downstream of the cylinder. Vortices shed alternately from both sides of the cylinder form into a

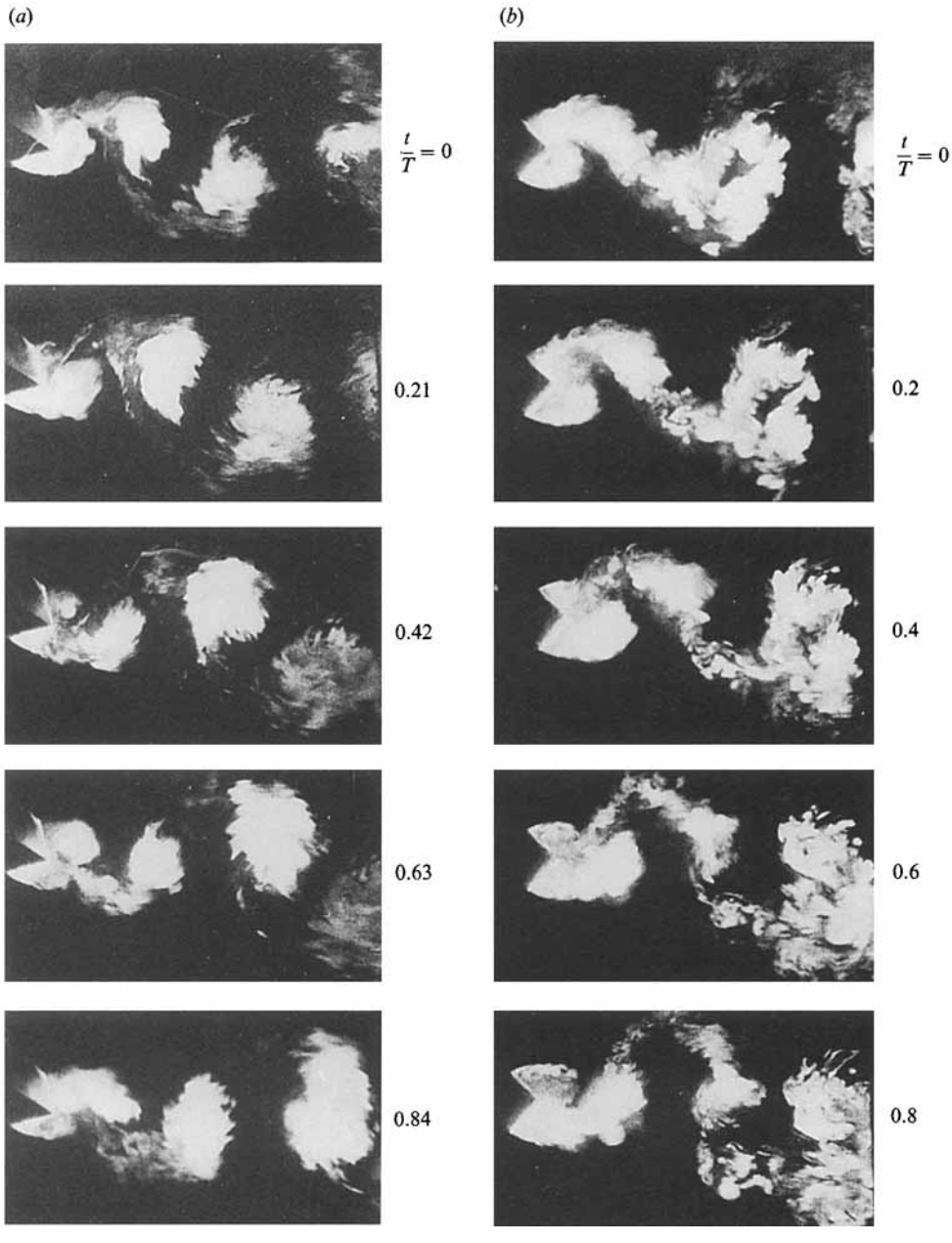

FIGURE 9(a, b). For caption see facing page.

familiar staggered arrangement downstream of the body. Note the relatively small spacing ratio of the vortex street, b/a, where b is the spacing between the two rows of vortices and a is the spacing between consecutive vortices in one row. The shedding was not always regular and for the case $\alpha = 15°$, an example of an instance where the shedding appears to be relatively weak in the viewed plane is shown in figure 7(*d*).

Figure 8 shows two types of flow pattern observed at $\alpha = 0°$ and $U/ND = 4.0$. The

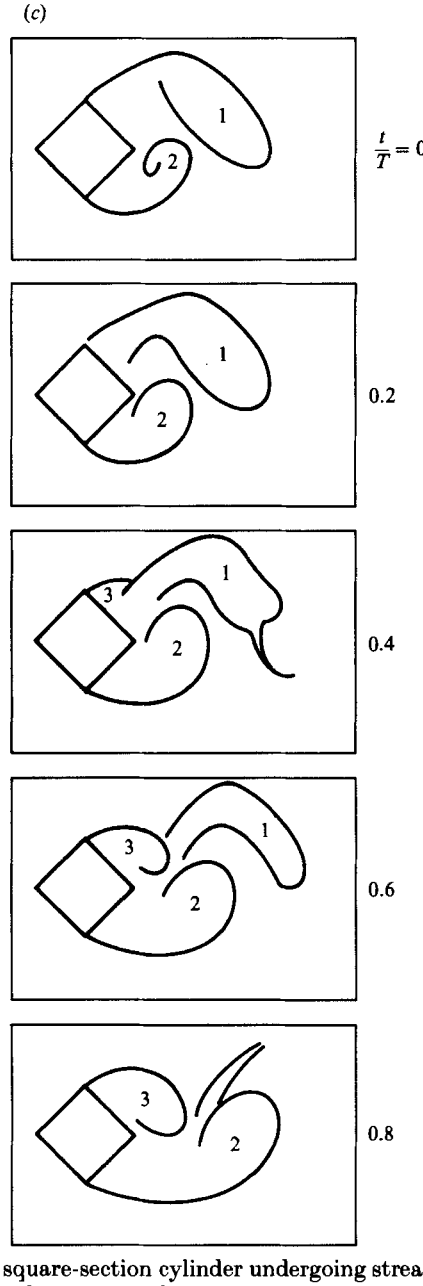

FIGURE 9. Vortex pattern for a square-section cylinder undergoing streamwise oscillations. T is the period and $t = 0$ when the cylinder is at its fully upstream position. (*a*) $\alpha = 15°$, $U/ND = 6.75$, $A_{rms}/D = 0.014$, $Re = 7.3 \times 10^3$. (*b*) $\alpha = 45°$, $U/ND = 4.54$, $Re = 4.9 \times 10^3$. (*c*) Sketches of vortex patterns at $\alpha = 45°$, $U/ND = 4.54$, $Re = 4.9 \times 10^3$. Recordings for cases (*b*) and (*c*) were made during the decay of streamwise oscillations.

r.m.s. value of the cylinder amplitude was about $0.03D$. In figure 8(*a*) vortices are shed simultaneously from both sides of the cylinder and the flow pattern is symmetric with respect to the wake centreline. One pair of contra-rotating vortices is shed in each cycle of the cylinder vibration; since $U/ND = 4.0$, this means that shedding occurs near twice the natural shedding frequency $n = SU/D$. The shedding

process is seen in figure 8(*a*) starting from an instant when the cylinder is near its fully upstream position ($t = 0$). Here, t is time and T is the period of the cylinder vibration. As the cylinder moves downstream, vortices roll-up close to the back face of the model. When the cylinder is moving upstream, the distance from the centre of the vortices to the back face increases and before the cylinder is at its full upstream position, the shear layers develop a neck which indicates that fluid is being sucked from outside the wake into the vortex formation region. The appearance of the neck marks the beginning of the development of a new vortex pair.

Photographs of the second of the two patterns recorded under the above conditions are shown in figure 8(*b*). Sketches of the flow pattern are presented in figure 8(*c*). Vortices of opposite sign are shed alternately, each side of the cylinder shedding one vortex every two cycles of the cylinder vibration. For $U/ND = 4.0$, this gives a shedding frequency that is very close to the stationary-cylinder value. A new vortex starts to develop close to the instant when the cylinder is at its fully upstream position. For example, figure 8(*c*) shows that vortex 3 starts to form in the upper shear layer when $t/T \approx 2.0$. When the vortex is forming, the vortex of opposite sign formed in the previous cycle, that is vortex 2, is elongated and split into two parts. One part (vortex 2*a*) stays on the same side of the wake and helps to form the next pair of contra-rotating vortices. The other part (vortex 2*b*) is drawn across the wake and forms a pair with the remnant of the vortex left behind when splitting occurred in the previous cycle. Further downstream of the body, vortex pairs are arranged on both sides of the wake centreplane in a staggered formation. The first three photographs of figure 8(*b*) and the first three sketches of figure 8(*c*) show the splitting of the upper shear-layer vortex. It appears that the upper shear layer starts to form a new vortex before the splitting of the old vortex is completed. The bottom photograph of figure 8(*b*) shows how vortex pairs are staggered in the wake.

For the combination of angle of incidence, reduced velocity, and cylinder amplitude examined above, the asymmetric vortex shedding mode was by far the dominant mode. About 240 cycles of the cylinder vibration were examined for $\alpha = 0°$, $U/ND = 4.0$, and $A_{\mathrm{rms}}/D = 0.03$, and only about one-fifth of the cycles belonged to the symmetric mode. The vortex shedding process switches between the symmetric and the antisymmetric modes without causing any significant change in the cylinder vibration amplitude. The time interval between two consecutive switches of the vortex pattern was not constant. For example, the number of consecutive cycles for which the asymmetric mode of shedding was maintained for the case considered ranged from about 3 to 67.

That, for a given flow condition, more than one mode of shedding is possible may be the reason why more than one vibration amplitude can be sustained at a given reduced velocity. As shown in figure 2, when the reduced velocity is increased from 4.0, the cylinder response can follow either a low- or a high-amplitude path. We suspect that the high-amplitude branch of the response curve is associated mainly with the symmetric shedding mode. It appears that to produce the high-amplitude response, the reduced velocity must be increased at an instant when the mode of shedding is symmetric.

For $\alpha = 0°$ and $U/ND = 4.0$, visualization was also performed when the cylinder r.m.s. amplitude was only about $0.007D$. The results are not shown because the flow pattern was similar to that of the stationary cylinder.

Figure 9(*a*) shows smoke patterns recorded at $\alpha = 15°$, $U/ND = 6.72$ and $A_{\mathrm{rms}}/D \approx 0.014$. Each side of the cylinder sheds a vortex every vibration cycle, and the mode of shedding and the configuration of the vortex wake are broadly similar

to those of the stationary cylinder. In figure 9(*a*), the model is orientated so that shear-layer reattachment occurs on the upper side face. Note that vortices start to form on that side of the wake close to the beginning of the half-cycle where the cylinder is moving downstream.

To gain more insight into the mechanism by which streamwise oscillation is sustained, we have visualized the wake of the vibrating cylinder under conditions where significant self-sustained oscillation does not occur. The experiment was performed at $\alpha = 45°$ and $U/ND = 4.54$. This reduced velocity is very close to $1/2S$ and vortices are expected to shed at half the vibration frequency. Streamwise vibration was imposed on the cylinder and the flow was filmed during the decay of the motion. Figure 9(*b*) shows smoke patterns starting from the instant when the cylinder is fully upstream. Corresponding sketches are presented in figure 9(*c*). As in the previous cases, a vortex (vortex 3 in figure 9*c*) first appears close to the instant when the cylinder reverses direction. However, unlike at $\alpha = 0°$ where the motion is self-sustained and a vortex starts to form close to the instant where the cylinder is fully upstream (see for example vortex 3 in figure 8*c*), the vortex appears close to the point where the cylinder is at its fully downstream position. This means that the vortex-induced forces are phase shifted by about 180° with respect to the self-sustained case at $\alpha = 0°$.

We have estimated the speed of the vortices, U_N, from the smoke patterns. Because it is difficult to ascertain the position of vortex centres, these results can only serve to give a rough estimate. In the stationary-cylinder case, our results indicate $U_N = 0.8U$ for $\alpha = 0°$ and 15°, and $0.7U$ for $\alpha = 45°$, U being the undisturbed stream velocity. These results seem quite reasonable considering Obasaju's (1983) report that at $Re = 10^4$, U_N ranged from 0.84 at $\alpha = 0°$ to 0.77 at $\alpha = 45°$. In the case of the oscillating model, we measured $U_N = 0.8U$ at $U/ND = 4.0$ and $\alpha = 0°$. For the symmetric mode of shedding therefore, the spacing between consecutive vortex pairs is about $3.2D$. For the alternate shedding mode, the spacing between consecutive pairs of split vortices lying on the same side of the wake is about $6.4D$.

4. Discussion of results

One of the objectives of this study is to identify the mechanisms of excitation leading to sustained streamwise oscillations of cylinders. For excitation to come about, the streamwise force (i.e. the instantaneous drag) must attain its minimum during the half-cycle when the cylinder is moving upstream. At $\alpha = 0°$, vortices were shown to shed when the cylinder is moving upstream. The shedding marks the beginning of the development of a new vortex and we suggest that this phase of the vortex shedding process is associated with minimum streamwise force.

There is another possible source of excitation, namely wake breathing, and this arises from the cylinder movements. When a body moves in an otherwise still fluid, fluid is displaced forward and outward ahead of the body whereas behind, fluid is drawn inwards to occupy the space vacated by the body. When the flow induced by the movement of a bluff body is combined with the separated flow generated by the stationary body when placed in a uniform stream, we expect the shear layers near the body to be tending to moving inwards (i.e. closer to the body) when the body is moving upstream and outwards when the body is moving downstream. Studies of the flow around stationary rectangular cylinders (Bearman & Trueman 1972) show that when a square-section cylinder is set at 0° incidence, bringing the shear layers closer to the body enhances the interaction between the shear layers and the trailing-edge

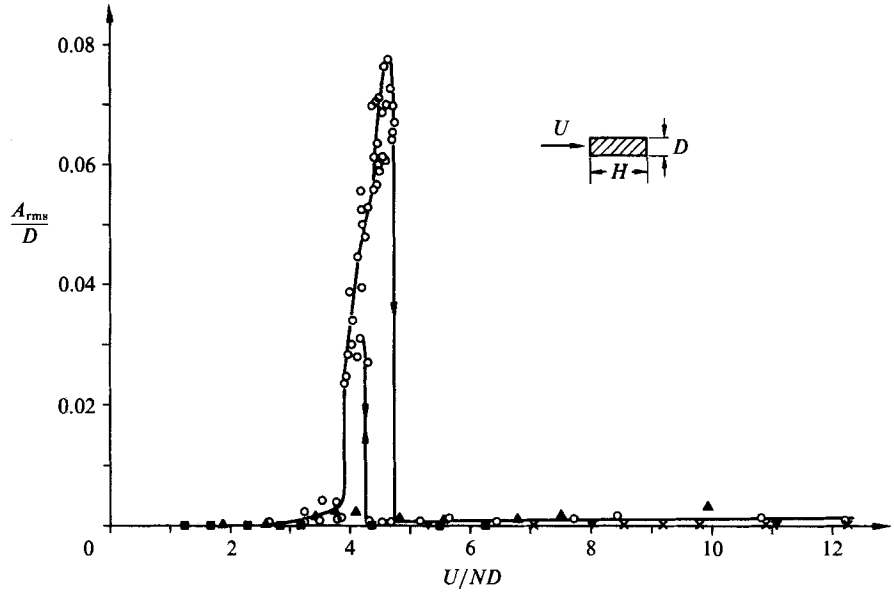

FIGURE 10. Root-mean-square value of cylinder amplitude, measured at $\alpha = 0°$, versus reduced velocity: ■, $H/D = 0.20$; ▲, $H/D = 0.25$; ○, $H/D = 1$; ×, $H/D = 4$; ▼, $H/D = 5$.

corners. The result is that vortices form further downstream and the drag is lower. Therefore when the cylinder is moving upstream, interaction between the shear layers and the trailing-edge corners may lead to a lower drag. Wake breathing could thus be a realistic mechanism of excitation.

Thus for $\alpha = 0°$ there are two possible sources of streamwise excitation besides buffeting: vortex shedding and wake breathing. The wake breathing is expected to sustain streamwise oscillations only where there is shear layer/trailing-edge corner interaction. In our experiments, regular streamwise oscillation occurs only around $U/ND = 1/2S$. This appears to suggest that the oscillation is vortex-induced. However, we have tested a number of rectangular cylinders and did not find sustained streamwise oscillation where there is vortex shedding but there appears to be no excitation by wake breathing. For example, in figure 10 we present measurements made with our apparatus using rectangular cylinders with side ratio $H/D = 0.2$, 0.25, 1, 4 and 5, where H is section depth in the stream direction and D is section width normal to the flow. Interaction between the shear layers and the trailing-edge corners (and hence wake-breathing excitation) is expected when $0.6 \leqslant H/D \leqslant 2.7$. Figure 10 shows that sustained streamwise oscillation was observed only with the square-section cylinder, that is the case $H/D = 1$. Such a result suggests that regular vortex shedding is not a sufficient condition for sustained streamwise oscillation.

When $\alpha > 0°$, streamwise forces are generated not only on the front and back faces of the cylinder but also on the side faces. Further experiments, probably including measurements of unsteady forces, would have to be made before addressing the question of excitation mechanism in this case.

Up till now, data for streamwise oscillations have been available only for the circular cylinder. For this case $1/2S \approx 2.5$, and when K_s is small (e.g. $K_s = 0.38$), oscillation is induced in two zones, $1.0 \leqslant U/ND \leqslant 2.5$ and $2.5 \leqslant U/ND \leqslant 4.0$. The

maximum amplitude of oscillation recorded in both zones is $A/D \leqslant 0.12$. As K_s increases the amplitude decreases faster in the first zone (i.e. $1.0 \leqslant U/ND \leqslant 2.5$) than in the second. For example, when $K_s = 0.96$, the maximum amplitude is about $0.02D$ for the first zone compared to $0.08D$ for the second (King, Prosser & Johns 1973; King 1974). It has been suggested (King 1977) that significant streamwise oscillations do not occur if $K_s > 1.2$. In our experiment $K_s = 1.6$, yet the square-section cylinders, maximum amplitude is similar to that recorded with the circular cylinder when $K_s = 0.38$. We did not find large-amplitude oscillation when U/ND is much less than $1/2S$ and, at some angles of incidence, the oscillation occurred near $U/ND = 1/S$. Our results indicate that the square-section-cylinder mean drag is attenuated during streamwise oscillation. By contrast, measurements made by Tanida, Okajima & Watanabe (1973) indicate that near $U/ND = 12S$, the mean drag experienced by a circular cylinder, which is undergoing streamwise oscillation, is higher than the stationary cylinder value.

Vortex-induced oscillation is a complex phenomenon central to which is an interaction between a body and its wake. We have a situation where the wake excites a body and the body vibrates and in turn modifies the wake. The interaction continues to change things until the damping of the vibrating system is balanced by the excitation, and a state of dynamic equilibrium is reached. The characteristics of this body–wake interaction have been described by Bearman (1984). They include the capture of the vortex shedding by the body frequency and an increase in the extent of the cylinder span over which the shedding process is correlated. The vortex pattern can change drastically. Depending on the shape of the cylinder, the base suction, the mean drag coefficient, and the strength of shed vortices, can be amplified or attenuated. Virtually all our knowledge of this interaction comes from experiments made with cylinders undergoing oscillations transverse to the flow. Since in our experiments oscillations occur in-line with the flow, it was decided to further investigate how the vortex wake is modified during streamwise oscillations. To achieve this objective a simple model of the vortex wake will be examined.

Starting with the stationary cylinder case where the classical von Kármán vortex street is formed, if the vortex street is represented by two parallel rows of staggered point vortices in an ideal fluid, it can be shown that:

$$C_D\left(\frac{nD}{U}\right) = \frac{4}{\pi}\left(1-\frac{U_s}{U}\right)\left(\frac{U_s}{U}\right)^2\left[\coth^2\left(\frac{\pi b}{a}\right)+\left(\frac{U}{U_s}-2\right)\frac{\pi b}{a}\coth\left(\frac{\pi b}{a}\right)\right]. \tag{1}$$

Herein, U_s is induced velocity, $U_N/U = 1-U_s/U$ is the vortex convection velocity, n is the frequency of vortex shedding, b is the spacing between the two rows of vortices, and a is the spacing between consecutive vortices in a row. b/a is the spacing ratio. Since we measured $U_N/U = 0.8$ at 0° incidence, values of $C_D(nD/U)$ have been calculated using $U_s/U = 0.2$. The results are plotted against b/a in figure 11. When $\alpha = 0°$ and the cylinder is stationary, $C_D = 2.2$ and $S = nD/U = 0.124$. Hence figure 11 predicts that either $b/a = 0.20$ or 0.56. Our photographs (figure 7) indicate that $b/a = 0.20$ is the right sort of value, so P in figure 11 is our starting point. Measurements made at 0° incidence suggest that when streamwise oscillation is induced C_D decreases while U_N/U remains constant. The oscillation occurs mainly when $U/ND > 1/2S$ and when vortices are shed alternately by the oscillating cylinder, $n = \frac{1}{2}N$. These considerations suggest that the oscillating-cylinder values of $C_D(nD/U)$ are less than the stationary cylinder value, and hence it is predicted that b/a is increased. According to figure 11, the classical von Kármán vortex street will

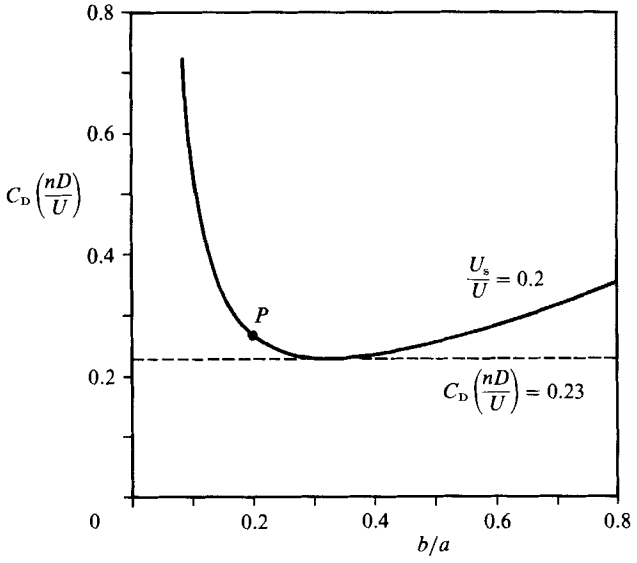

FIGURE 11. $C_D(nD/U)$, calculated from the vortex-street drag formula (equation (1)), versus spacing ratio.

not form when $C_D(nD/U)$ falls below 0.23. At $\alpha = 0°$ we measured $C_D = 1.0$ when $U/ND = 4.0$. When vortices are shed alternately, the corresponding value of nD/U is 0.125. So we get $C_D(nD/U) = 0.125$ which is less than 0.23. The relevant photographs are shown in figure 8, and it is seen that the classical von Kármán vortex street is not formed.

It is interesting that in the case of the circular cylinder where the mean drag of the oscillating cylinder is higher than the stationary-cylinder value, the above model predicts that b/a decreases during streamwise oscillation. Flow visualization by Griffin & Ramberg (1976) appears to confirm this finding.

The above model predicts that the strength of each vortex, Γ, is given by

$$\frac{\Gamma}{\pi UD} = \frac{2}{\pi}\left(\frac{U_s}{U}\right)\frac{a}{D}\coth\left(\frac{\pi b}{a}\right). \tag{2}$$

Considering again the case where U_N/U is constant and $U/ND = 4.0$, our prediction that b/a is increased during streamwise oscillation leads to the conclusion that vortex strength is attenuated. The same conclusion is reached by calculating the ratio of the circulation shed during the formation of a vortex by an oscillating body to that by a stationary body. Following Bearman & Obasaju (1982), the ratio is $[(1-C_{pb})_o/(1-C_{pb})_s]SU/n_oD$, where S is the stationary-body Strouhal number, n is the frequency of vortex shedding and the suffices o and s refer to oscillating and stationary cylinders, respectively. We have used $S = 0.125$ for $C_{pb} = -1.4$ for the stationary cylinder, and $C_{pb} = -0.2$ at $U/ND = 4.0$ for the oscillating cylinder. When the mode of shedding is symmetric, $n_o = N$ and the ratio of shed circulation is 0.25 which suggests that, for the symmetric shedding mode, the vortex strength is about $\frac{1}{4}$ of the stationary-cylinder value. When the shedding is antisymmetric, $n_o = \frac{1}{2}N$ but a shed vortex is split into two parts. Therefore it is estimated that a split vortex has about $\frac{1}{4}$ the strength of a stationary-cylinder vortex. A second estimate of the vortex strength was obtained for the symmetric mode by idealizing the wake

as two parallel rows of point vortices, a vortex of one row being exactly opposite a vortex of the other row. For this configuration, the vortex strength is (Kochin, Kibel & Rozel 1964) given by

$$\frac{\Gamma}{\pi UD} = \frac{2}{\pi}\left(\frac{U_s}{U}\right)\frac{a}{D}\tanh\left(\frac{\pi b}{a}\right). \tag{3}$$

Using $U_s/U = 0.2$, $a/D = 3.0$ and $b/D = 1$, (3) gives $\Gamma/\pi UD = 0.3$. In the case of the stationary model, (2) with $b/a = 0.2$, $a/D = 6$ and $U_s/U = 0.2$ gives $\Gamma/\pi UD = 1.4$. Hence for the symmetric shedding mode, vortex strength is estimated to be attenuated by a factor of 4.7.

Since it is sometimes supposed that vortex strength is magnified when vortex-induced oscillations occur, the above finding may seem paradoxical. However, if the vibrating system is represented by a linear second-order system, it can be shown that if the phase angle by which the oscillating drag leads the cylinder displacement is $\frac{1}{2}\pi$, then for $K_s = 1.6$ and $U/ND = 4.7$ a vibration amplitude of up to $0.12D$ can be sustained by an oscillating drag coefficient of only 0.08. For a stationary square-section cylinder in smooth flow, the coefficient of the fluctuating drag is (e.g. Lee 1975) about 0.2 at 0° incidence. This shows that the oscillation observed in our experiments can be wholly sustained by a vortex-induced force (and hence a vortex strength) which is less than the stationary-cylinder value.

As shown in figure 8(*b*), one of the modes in which shed vorticity convects away from a bluff body is by forming two rows of contra-rotating vortices. For a circular cylinder, such a street has been photographed by Griffin & Ramberg (1976) and it is one of the modes of vortex convection listed by Ongoren & Rockwell (1988) and by Williamson & Roshko (1988). Such a wake can also be formed by an elongated sharp-edged bluff prism (see for example Nakamura & Nakashima 1986), and this arrangement of vortices was classified (Steiner & Perry 1987) as a double-sided mushroom structure. We have used the term 'splitting' to describe the shedding process because it appears that the vortices are formed in the manner described by Freymuth, Bank & Palmer (1985). However, it is possible that what we refer to as splitting is actually the separation of the centres of two vortices. According to this interpretation, even during the antisymmetric shedding, the velocity field still has a symmetrical part (associated with wake breathing) which produces a weak pair of contra-rotating vortices every vibration cycle. Together with the alternate vortex shedding near $U/ND = 1/2S$, therefore, there may be an agglomeration of two vortices on one side of the cylinder which becomes obvious only later on.

5. Conclusions

The streamwise oscillation of a spring-mounted square-section cylinder set at angle of incidence, α, in the range from 0° to 45° has been investigated in the reduced-velocity range $3 < U/ND < 13$. The mass-damping parameter, K_s, of the vibrating system is 1.6 and measurements are made in the range of Reynolds number, Re, from 3.2×10^3 to 1.4×10^4.

Vortex-induced oscillations occur in narrow ranges of reduced velocity near $1/S$ and $1/2S$ (where S is the Strouhal number for the stationary body) and a root-mean-square vibration amplitude up to about $0.09D$ is recorded at $\alpha = 2.5°$. For $0° \leqslant \alpha < 13.5°$, oscillations occur mainly when U/ND is close to $1/2S$. By contrast for $\alpha \geqslant 13.5°$, where the configuration of the shear layers is more antisymmetrical owing to reattachment of one of the layers, streamwise oscillations occur mainly near $1/S$.

At $\alpha = 0°$, there are two possible sources of excitation besides buffeting, namely vortex shedding and wake breathing. The vortices help to sustain oscillations by adjusting their development so that shedding occurs when the cylinder is moving upstream. During oscillation, the cylinder steady-drag coefficient, C_D, can drop to 1.0, which is less than half the stationary-cylinder value. Three modes of vortex shedding have been identified. When the oscillation amplitude is small (e.g. root-mean-square amplitude of about $0.007D$) vortices of opposite sign are shed alternately and the familiar von Kármán vortex street is formed. For a root-mean-square amplitude of $0.03D$ and a reduced velocity of 4.0, a symmetric and an antisymmetric mode of shedding have been identified. In the symmetric mode, a pair of vortices is shed simultaneously and symmetrically every vibration cycle. In the antisymmetric mode, each side of the cylinder sheds a vortex every two vibration cycles and, when a vortex is forming on one side, it appears that the vortex shed in the previous vibration cycle by the other side is stretched and split into two parts. Split vortices of opposite sign then form a vortex street having a double-sided mushroom structure.

Analysis, done to help interpret the results, suggests that the spacing ratio of the vortex street is increased during streamwise oscillation. It is estimated that the strength of shed vortices can drop to about $\frac{1}{4}$ of the stationary-cylinder value.

The research was carried out at the Institute of Hydromechanics, University of Karlsruhe, West Germany, and was supported by the German Science Foundation (DFG) through SFB 210. E. D. Obasaju would like to thank Professor E. Naudascher for making his visit possible and the staff of the Institute of Hydromechanics for providing a friendly and stimulating working environment. We would like to thank The City University for granting E. D. Obasaju a leave of absence.

REFERENCES

Bearman, P. W. 1984 Vortex shedding from oscillating bluff bodies. *Ann. Rev. Fluid Mech.* **16**, 195–222.

Bearman, P. W., Downie, M. J., Graham, J. M. R. & Obasaju, E. D. 1985 Forces on cylinders in viscous oscillatory flow at low Keulegan–Carpenter numbers. *J. Fluid Mech.* **104**, 337–356.

Bearman, P. W. & Obasaju, E. D. 1982 An experimental study of pressure fluctuations on fixed and oscillating square-section cylinders. *J. Fluid Mech.* **119**, 297–321.

Bearman, P. W. & Trueman, D. M. 1972 An investigation of the flow around rectangular cylinders. *Aeronaut. Q.* **23**, 229–237.

Ermshaus, R., Knisely, C. & Naudascher, E. 1985 Flow visualisation in the wake of three-dimensional bodies undergoing self-sustained oscillations. In *Optical Methods in Dynamics of Fluids and Solids* (ed. M. Pichal). Springer.

Ermshaus, R., Naudascher, E. & Obasaju, E. D. 1986 Stromungserregte Schwingungen zylindrischer und axialsymmetrischer Körper in Strömungsrichtung. *Bericht Nr.* SFB 210/E/25. Universität Karlsruhe, W. Germany.

Freymuth, P., Bank, W. & Palmer, M. 1985 Further experimental evidence of vortex splitting. *J. Fluid Mech.* **152**, 289–299.

Griffin, O. M. & Ramberg, S. E. 1976 Vortex shedding from a cylinder vibrating in line with an incident uniform flow. *J. Fluid Mech.* **75**, 257–271.

King, R. 1974 Vortex excited structural oscillations of a circular cylinder in steady currents. *Offshore Tech. Conf. Paper* OTC 1948.

King, R. 1977 A review of vortex shedding research and its application. *Ocean Engng* **4**, 141–171.

King, R., Prosser, M. J. & Johns, D. J. 1973 On vortex excitation of model piles in flowing water. *J. Sound Vib.* **29**, 169–188.

KNISELY, C. W. 1985 Strouhal numbers of rectangular cylinders at incidence. *Rep.* SFB 210/E/13, Universität Karlsruhe, W. Germany.

KOCHIN, N. E., KIBEL, I. A. & ROZEL, N. V. 1964 *Theoretical Hydromechanics*, p. 218. Interscience.

LEE, B. E. 1975 The effect of turbulence on the surface pressure field of a square prism. *J. Fluid Mech.* **69**, 263–282.

NAKAMURA, Y. & NAKASHIMA, M. 1986 Vortex excitation of prisms with elongated rectangular, H and cross-sections. *J. Fluid Mech.* **163**, 149–169.

NAUDASCHER, E. 1987 Flow-induced streamwise vibration of structures. *J. Fluids Structures* **1**, 265–298.

OBASAJU, E. D. 1983 An investigation of the effects of incidence on the flow around a square section cylinder. *Aeronaut. Q.* **34**, 243–259.

ONGOREN, A. & ROCKWELL, D. 1988 Flow structure from an oscillating cylinder. Part 2. Mode competition in the near wake. *J. Fluid Mech.* **191**, 225–245.

SCHMITT, F. & RUCK, B. 1986 Laserlichtschnittverfahren zur qualitativen Strömungsanalyse. *Laser Optoelektronik*, Nr. 2. Stuttgart: AT-Fachverlag.

STEINER, T. R. & PERRY, A. E. 1987 Large-scale vortex structures in turbulent wakes behind bluff bodies. Part 2. Far-wake structures. *J. Fluid Mech.* **174**, 271–298.

TANIDA, Y., OKAJIMA, A. & WATANABE, Y. 1973 Stability of a circular cylinder oscillating in uniform flow or in a wake. *J. Fluid Mech.* **61**, 769–784.

WILLIAMSON, C. H. K. & ROSHKO, A. 1988 Vortex formation in the wake of an oscillating cylinder. *J. Fluids Structures* **2**, 355–381.